Copy 5
RM L56B14

NACA

RESEARCH MEMORANDUM

EFFECTS OF REYNOLDS NUMBER AND LEADING-EDGE SHAPE ON THE LOW-SPEED LONGITUDINAL STABILITY OF A 6-PERCENT-THICK 45° SWEPTBACK WING

By William C. Schneider

Langley Aeronautical Laboratory
Langley Field, Va.

CLASSIFIED DOCUMENT

NATIONAL ADVISORY COMMITTEE
FOR AERONAUTICS

WASHINGTON

April 18, 1956

NATIONAL ADVISORY COMMITTEE FOR AERONAUTICS

RESEARCH MEMORANDUM

EFFECTS OF REYNOLDS NUMBER AND LEADING-EDGE SHAPE ON THE LOW-SPEED LONGITUDINAL STABILITY OF A 6-PERCENT-THICK 45° SWEPTBACK WING

By William C. Schneider

SUMMARY

Force-test data showing the effects of changes in leading-edge radius (nose shape) on the low-speed longitudinal stability of a 6-percent-thick 45° sweptback wing of aspect ratio 3 are presented for several ranges of Reynolds number and Mach number. Data are presented for wings with NACA 0006-(4.76)3, NACA 0006-(6.74)3, and modified NACA 0006-(3.88)3 airfoil sections with leading-edge radii of 0.0025, 0.0050, and 0.0025 of the local wing chord parallel to the plane of symmetry, respectively, and for Reynolds numbers up to 6.6×10^6 and Mach numbers up to 0.20. This study is a continuation of the studies published in NACA RM L55F06, NACA RM L55H04, and NACA RM L55L30.

The results indicated that, as the airfoil sections were thinned at the nose, separation effects occurred at lower values of lift coefficient. Increasing the test Reynolds number delayed somewhat the onset of separation effects.

INTRODUCTION

As part of a generalized study of the stalling of sweptback wings, a systematic investigation is being conducted to provide data on the effects of leading-edge radius on the longitudinal stability characteristics of a series of wings with varying thickness ratio, thickness distribution, camber, aspect ratio, and sweep angle. (See refs. 1, 2, and 3.) The present paper reports the results of tests of a 45° sweptback wing with an aspect ratio of 3, and 6-percent-thick airfoil sections. The airfoil section was modified systematically to study the effects of leading-edge shape on the static longitudinal stability characteristics. Tests were conducted at atmospheric pressure and at 33 pounds per square inch absolute pressure, which permitted Reynolds number ranges from

1.3×10^6 to 4.1×10^6 (Mach number from 0.06 to 0.20) and from 2.3×10^6 to 6.6×10^6 (Mach numbers from 0.05 to 0.15), respectively.

SYMBOLS

C_L	lift coefficient, Lift/qS
$C_{L_{inf_s}}$	inflection lift coefficient with stable change in pitching moment, $\left(-\frac{dC_m}{dC_L} \text{ increasing}\right)$
$C_{L_{inf_u}}$	inflection lift coefficient with unstable change in pitching moment, $\left(-\frac{dC_m}{dC_L} \text{ decreasing}\right)$
$C_{L_{max}}$	maximum lift coefficient
C_m	pitching-moment coefficient about $0.25\bar{c}$, Pitching moment/$qS\bar{c}$
S	wing area, sq ft
$\bar{c}$	mean aerodynamic chord, $\frac{2}{S}\int_0^{b/2} c^2 dy$, ft
c	local wing chord parallel to plane of symmetry, ft
y	spanwise coordinate normal to plane of symmetry, ft
b	wing span, ft
q	free-stream dynamic pressure, $\frac{1}{2}\rho V^2$, lb/sq ft
ρ	density of air, slugs/cu ft
V	free-stream velocity, ft/sec
R	Reynolds number
M	Mach number

[redacted]

$\Lambda_{c/4}$ sweepback of quarter-chord line, deg

A aspect ratio, b^2/S

x chordwise coordinate of airfoil section, ft

z vertical coordinate of airfoil section, ft

MODEL

The wings tested during this investigation had the following geometric characteristics: aspect ratio, 3; 45° sweepback of the quarter-chord line; taper ratio of 0.5; and a maximum thickness ratio of 6 percent chord. (See fig. 1.) Three airfoil sections were tested: NACA 0006-(4.76)3, NACA 0006-(6.74)3, and a modified NACA 0006-(3.88)3. (Coordinates for the three airfoil sections are listed in fig. 2.) The first two sections were formed by modifying the standard NACA four-digit airfoil by the procedure outlined in reference 4 in such a manner that the leading-edge radii were 0.25 percent c and 0.50 percent c, respectively. For the third airfoil, the standard procedure was used to form the NACA 0006-(3.88)3 airfoil section from 0.4 percent of the chord aft. The forward 0.4 percent was formed by fairing the airfoil with the leading-edge radius of 0.25 percent c, instead of the normal 0.167 percent c for that airfoil. The resulting airfoil will be designated herein as an NACA 0006-(3.88)3 modified airfoil section.

Wing	$\Lambda_{c/4}$	Aspect ratio	Taper ratio	Leading-edge radius	Airfoil section
1	45	3	0.5	0.0025c	NACA 0006-(4.76)3
2	45	3	0.5	0.0050c	NACA 0006-(6.74)3
3	45	3	0.5	0.0025c	NACA 0006-(3.88)3 (mod.)

TESTS AND CORRECTIONS

Tests

Tests were conducted at a tunnel pressure of 33 pounds per square inch absolute for all three wings and at atmospheric pressure for the wings with NACA 0006-(6.74)3 and NACA 0006-(3.88)3 modified airfoil

sections. The following Mach number and Reynolds number variations resulted as the models were tested through a large part of the tunnel speed range:

Tunnel pressure, lb/sq in. abs	Variation of Reynolds number	Variation of Mach number
14.7 (atmospheric)	1.3×10^6 to 4.1×10^6	0.064 to 0.20
33	2.3×10^6 to 6.6×10^6	0.05 to 0.15

The model was supported on the normal two-support system of the Langley 19-foot pressure tunnel.

Corrections

The pitching-moment data and values of angle of attack have been corrected for tunnel-wall effects by the method of reference 5. These corrections are

$$\Delta\alpha = 0.967C_L$$

$$\Delta C_m = 0.00392C_L$$

Since primary interest in these data was centered on the variation of the lift and pitching moments rather than on their absolute values, tests to determine the model-support tare and interference effects were not conducted. However, the zero-lift pitching-moment coefficient and the angle of attack at zero lift on a wing with no camber, twist, or dihedral were taken as an indication of the combined effects of model-support tare and interference, air-stream misalinement, and model asymmetry. These corrections were assumed to be independent of lift coefficient, and the lift and pitching-moment curves were shifted by the average value of the zero-lift pitching moment and angle of attack as a first-order approximation.

RESULTS AND DISCUSSION

The variations of lift and pitching-moment coefficient with angle of attack are presented in figures 3 to 5 and the variations of pitching-moment coefficient with lift are presented in figures 6 to 8.

The effects of variation in airfoil section on the pitching-moment characteristics of the wings are shown in figure 9, whereas the effects of changes in Reynolds number are illustrated in figure 10. Mach number effects for two of the wings are shown in figure 11. The variations of $C_{L_{inf_u}}$, $C_{L_{inf_s}}$, and $C_{L_{max}}$ with Reynolds number are shown in figures 12, 13, and 14 for the wings with the various airfoil sections. The quantities $C_{L_{inf_u}}$ and $C_{L_{inf_s}}$ are used to designate the lift coefficient beyond which there is a marked change in the pitching-moment characteristics, $C_{L_{inf_u}}$ denoting an unstable change and $C_{L_{inf_s}}$ denoting a stable change. In figure 13, two values of $C_{L_{inf_s}}$ are shown for the data obtained at 33 pounds per square inch absolute, since the force data show the pitching moment to have two successive stable shifts.

Changing the nose shape of the 6-percent-thick airfoil had considerable effect on the pitching-moment characteristics of the wings. (See fig. 9.) As the airfoil sections of the wing were thinned at the nose, the separation effects occurred at lower values of lift coefficient, as evidenced by the lower values of $C_{L_{inf_u}}$. A comparison of figures 12 and 14 shows that the values of $C_{L_{inf_s}}$ for the two wings with leading-edge radius of 0.0025c are almost identical through the Reynolds number range. The unstable break $C_{L_{inf_u}}$ is not similar for the two wings, in that the effect of thinning the section behind the nose was a lessening of the Reynolds number effects, thereby lowering the value to a marked degree at the higher Reynolds numbers.

Increasing the Reynolds number at a constant Mach number generally increased both $C_{L_{inf_u}}$ and $C_{L_{inf_s}}$ for the wing with an NACA 0006-(6.74)3 airfoil section. (See fig. 10(a).) For the wing with NACA 0006-(3.88)3 modified airfoil sections, the effect of Reynolds number was somewhat less marked for the unstable break than for $C_{L_{inf_s}}$. (See fig. 10(b).)

The effects of an independent change in Mach number are shown in figures 11(a) and 11(b). Little effect is noted for either wing. The

most significant change at the higher Mach numbers is the elimination of the slight stable shift in the pitching moment which occurred at low lift coefficients for the wing with the larger radius. (See figs 11 and 13.)

The effects of leading-edge radius and Reynolds number on the maximum lift coefficient can be seen to be small for these wings. (See figs. 12, 13, and 14.)

Langley Aeronautical Laboratory,
National Advisory Committee for Aeronautics,
Langley Field, Va., January 31, 1956.

REFERENCES

1. Foster, Gerald V., and Schneider, William C.: Effects of Leading-Edge Radius on the Longitudinal Stability of Two 45° Sweptback Wings As Influenced by Reynolds Numbers Up to 8.20×10^6 and Mach Numbers Up to 0.303. NACA RM L55F06, 1955.

2. Foster, Gerald V.: Effect of Leading-Edge Radius on the Longitudinal Stability of Two 45° Sweptback Wings Incorporating Leading-Edge Camber As Influenced by Reynolds Numbers Up to 8.00×10^6 and Mach Numbers Up to 0.290. NACA RM L55H04, 1955.

3. Schneider, William C.: Effects of Leading-Edge Radius on the Longitudinal Stability Characteristics of Two 60° Sweptback Wings At High Reynolds Numbers. NACA RM L55L30, 1956.

4. Stack, John, and Von Doenhoff, Albert E.: Tests of 16 Related Airfoils at High Speeds. NACA Rep. 492, 1934.

5. Sivells, James C., and Salmi, Rachel M.: Jet-Boundary Corrections for Complete and Semispan Swept Wings in Closed Circular Wind Tunnels. NACA TN 2454, 1951.

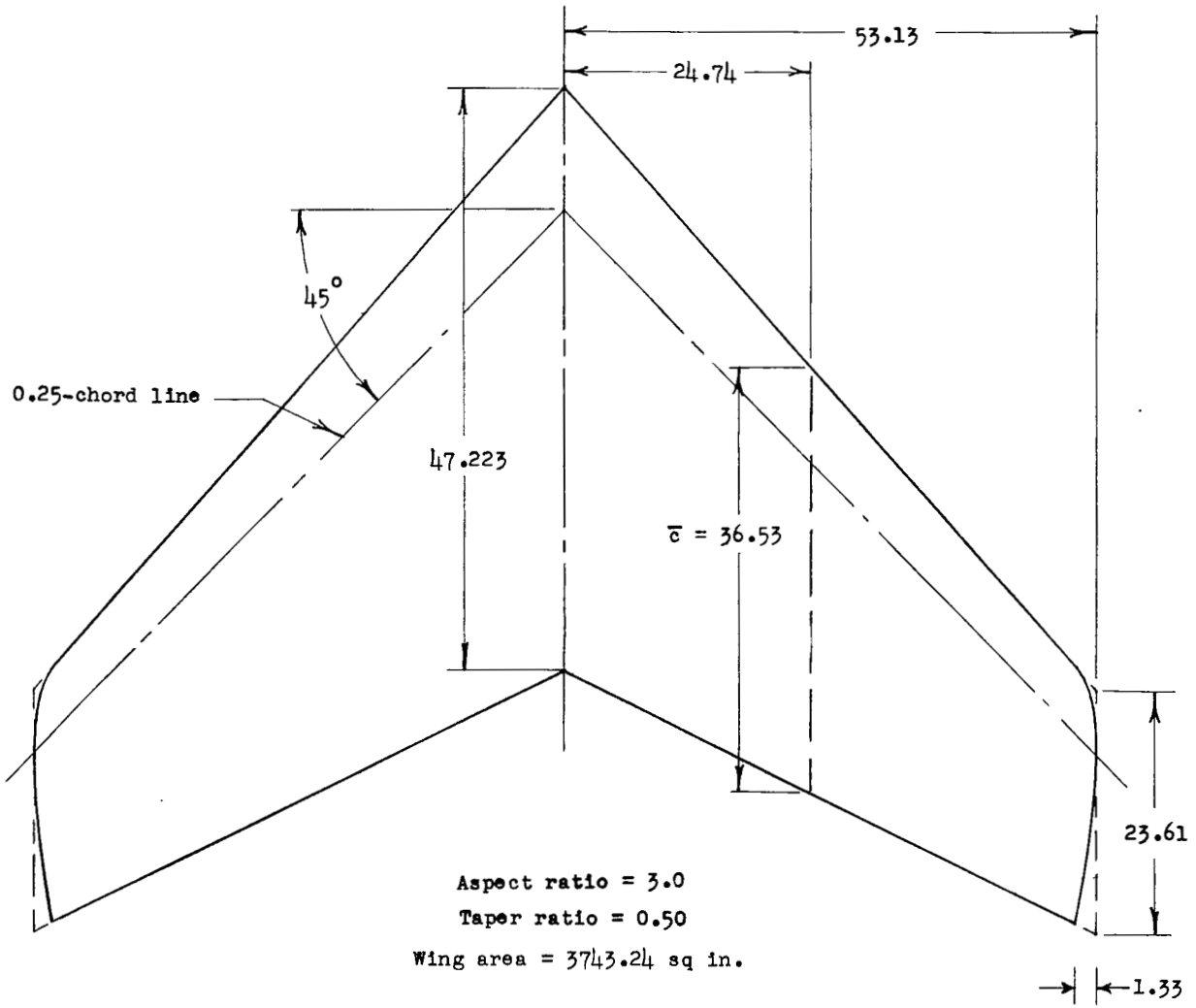

Figure 1.- Details of wings. All dimensions in inches unless otherwise noted.

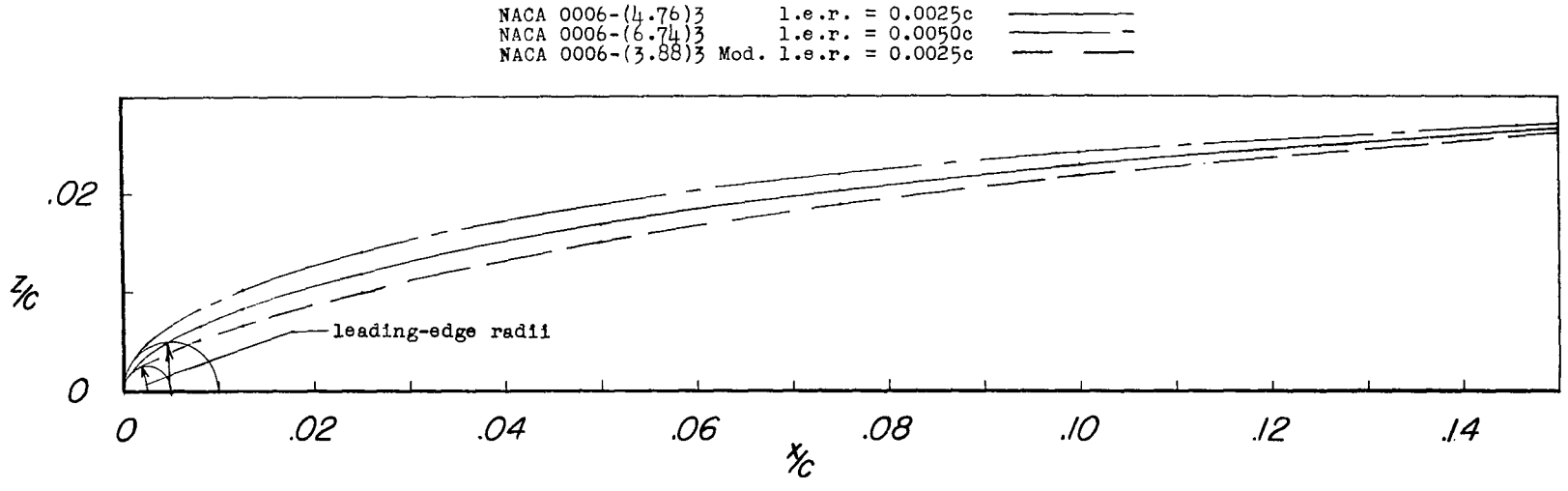

Ordinates of airfoils

NACA airfoil	0006-(4.87)3	0006-(6.74)3	.0006-(3.88)3 Mod.
L.E. radius	0.0025c	0.0050c	0.0025c
$\frac{x}{c}$	$\frac{z}{c}$	$\frac{z}{c}$	$\frac{z}{c}$
0	0	0	0
.0125	.0083	.0103	.0066
.0250	.0119	.0141	.0100
.0500	.0168	.0189	.0151
.0750	.0203	.0220	.0190
.1000	.0230	.0243	.0220
.1500	.0267	.0273	.0263
.2000	.0288	.0289	.0286
.3000	.0300	.0300	.0300
.4000	.0292	.0292	.0292
.5000	.0271	.0271	.0271
.6000	.0236	.0236	.0236
.7000	.0191	.0191	.0191
.8000	.0136	.0136	.0136
.9000	.0074	.0074	.0074
1.000	.0006	.0006	.0006

Figure 2.- Coordinates of airfoil sections.

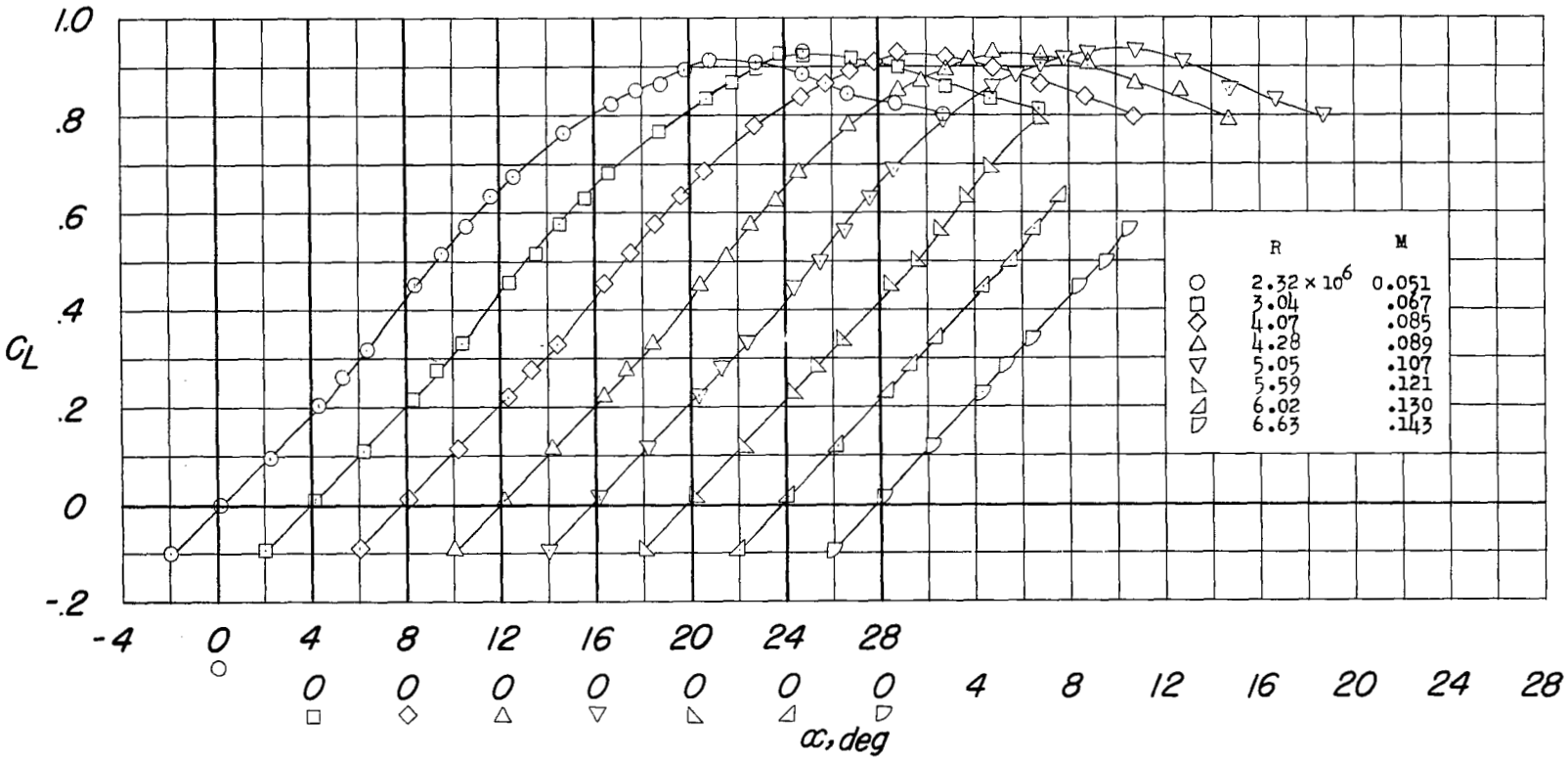

(a) C_L against α.

Figure 3.- Variation of lift and pitching-moment coefficients with angle of attack for a 45° sweptback wing with aspect ratio of 3 and NACA 0006-(4.76)3 airfoil sections. Leading-edge radius, 0.0025; tunnel pressure of 33 pounds per square inch, absolute.

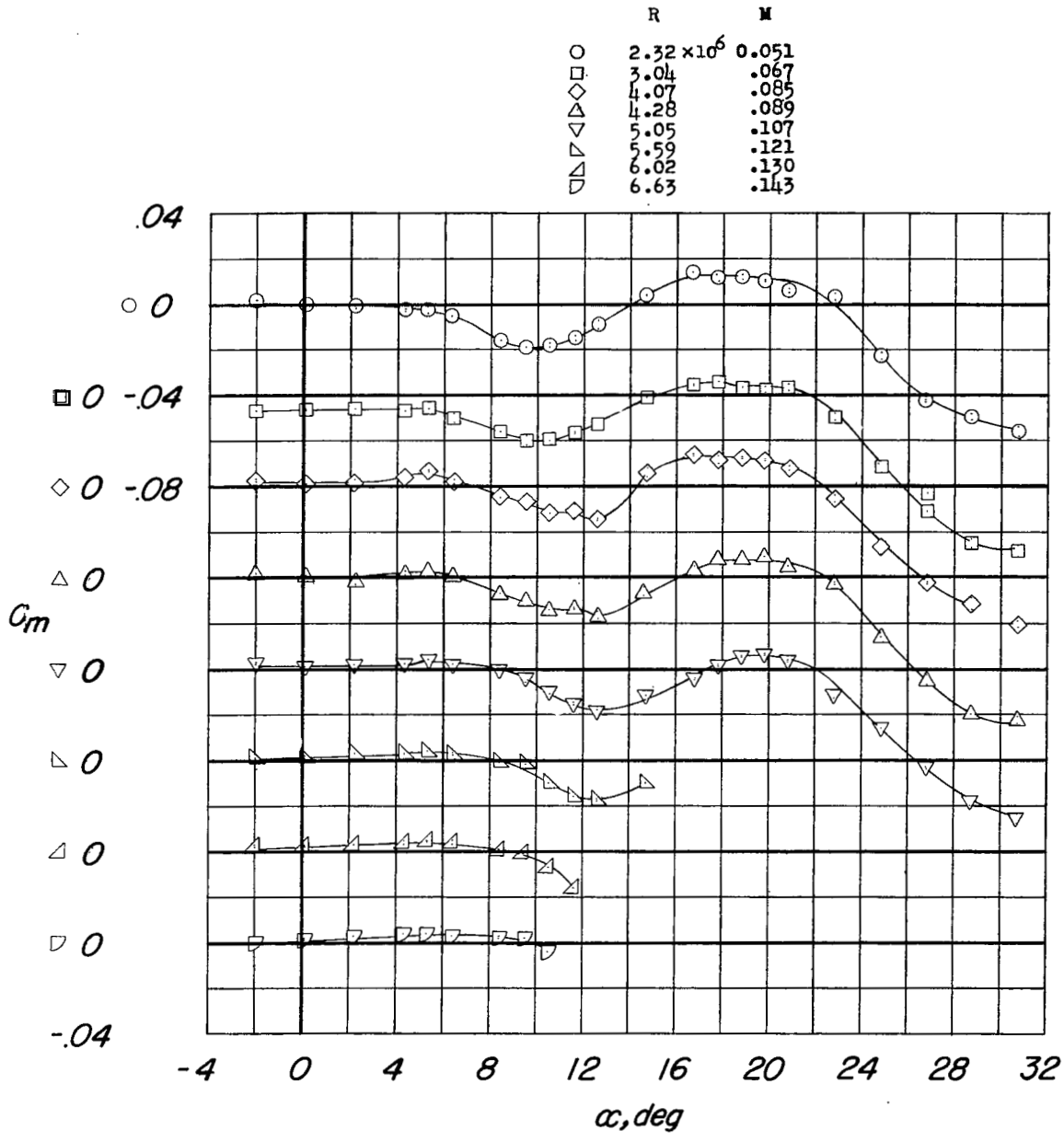

(b) C_m against α.

Figure 3.- Concluded.

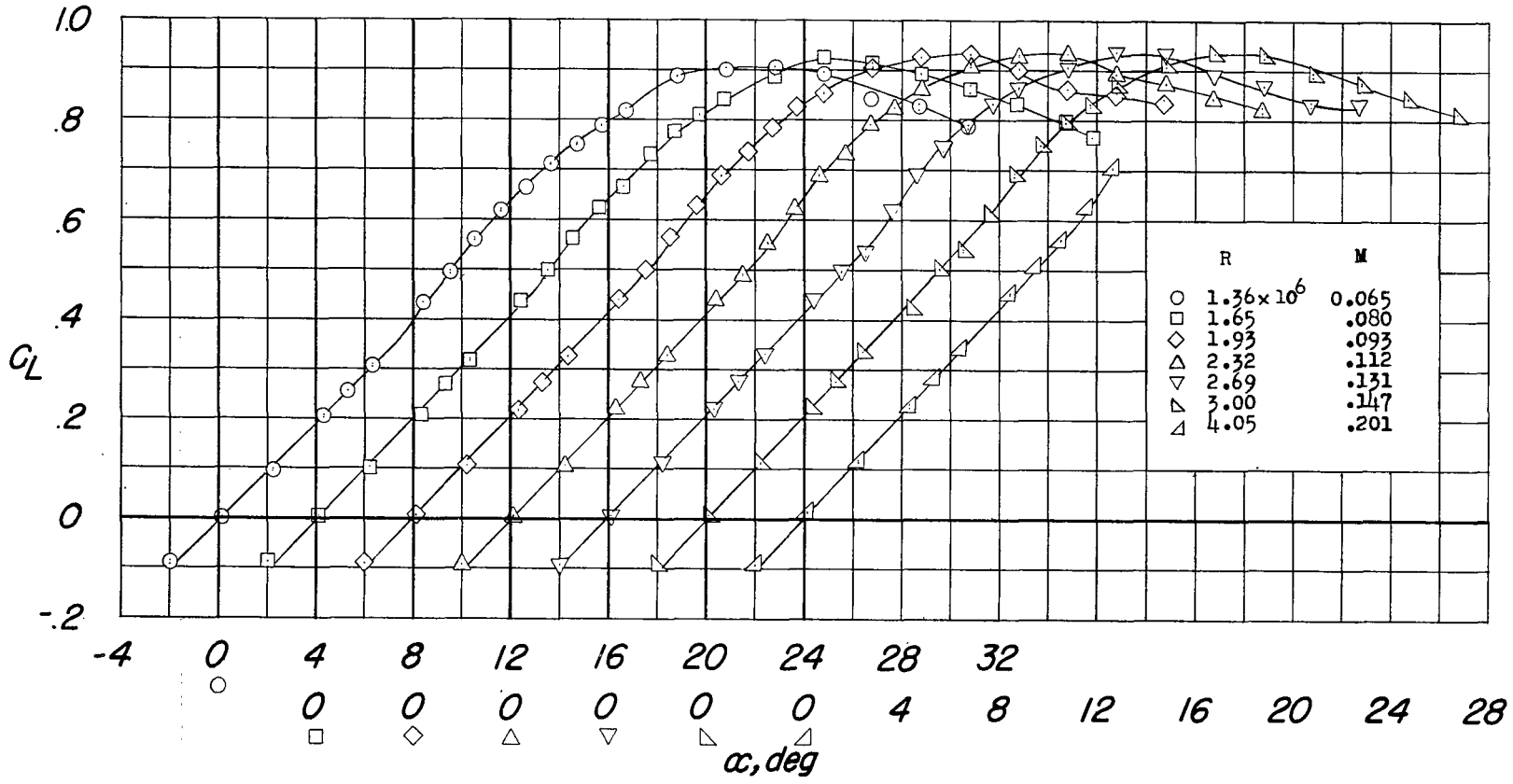

(a) C_L against α; tunnel pressure, atmospheric.

Figure 4.- Variation of lift and pitching-moment coefficients with angle of attack of a 45° sweptback wing with aspect ratio of 3 and NACA 0006-(6.74)3 airfoil sections. Leading-edge radius, 0.0050.

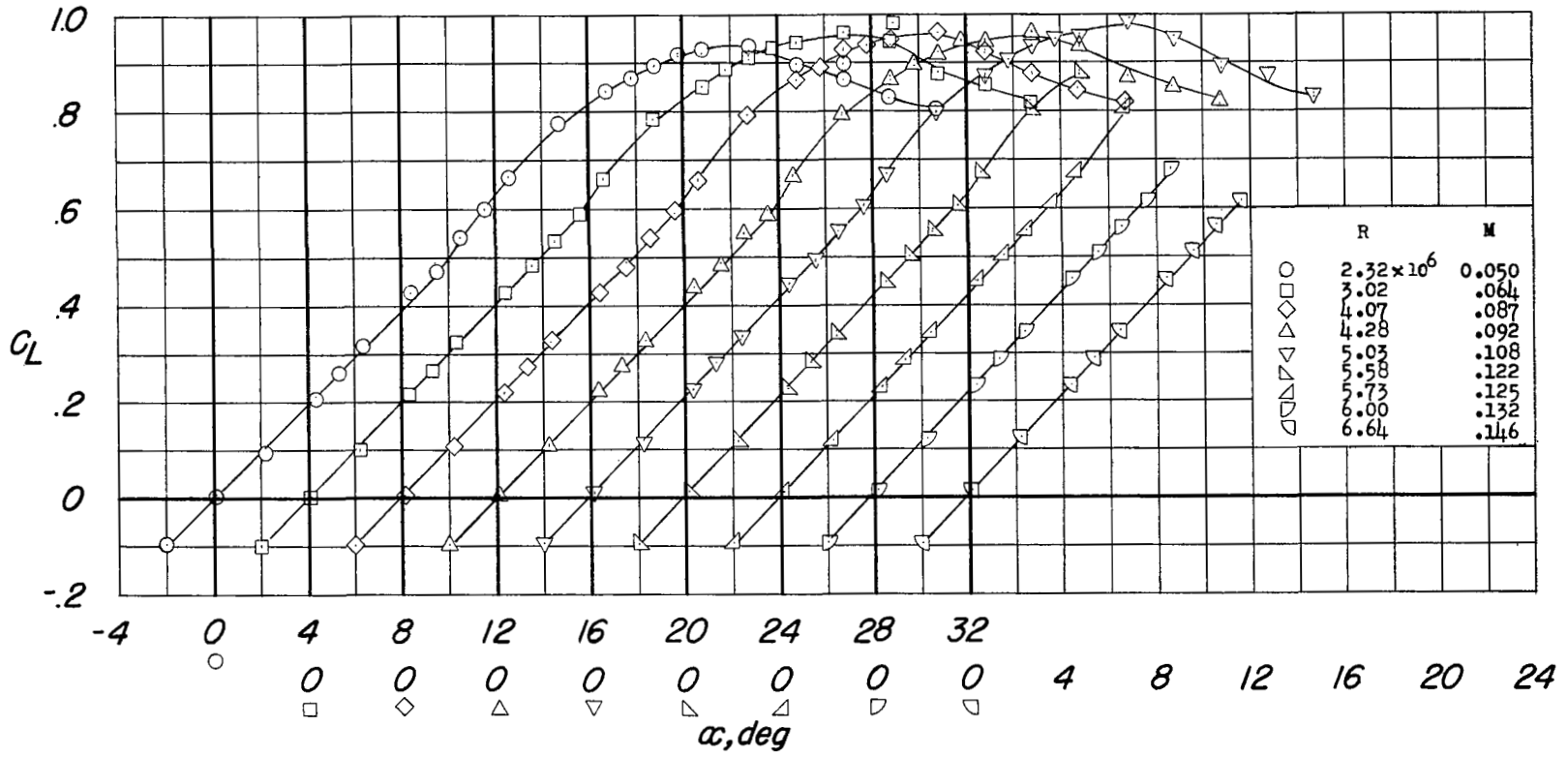

(b) C_L against α; tunnel pressure, 33 pounds per square inch, absolute.

Figure 4.- Continued.

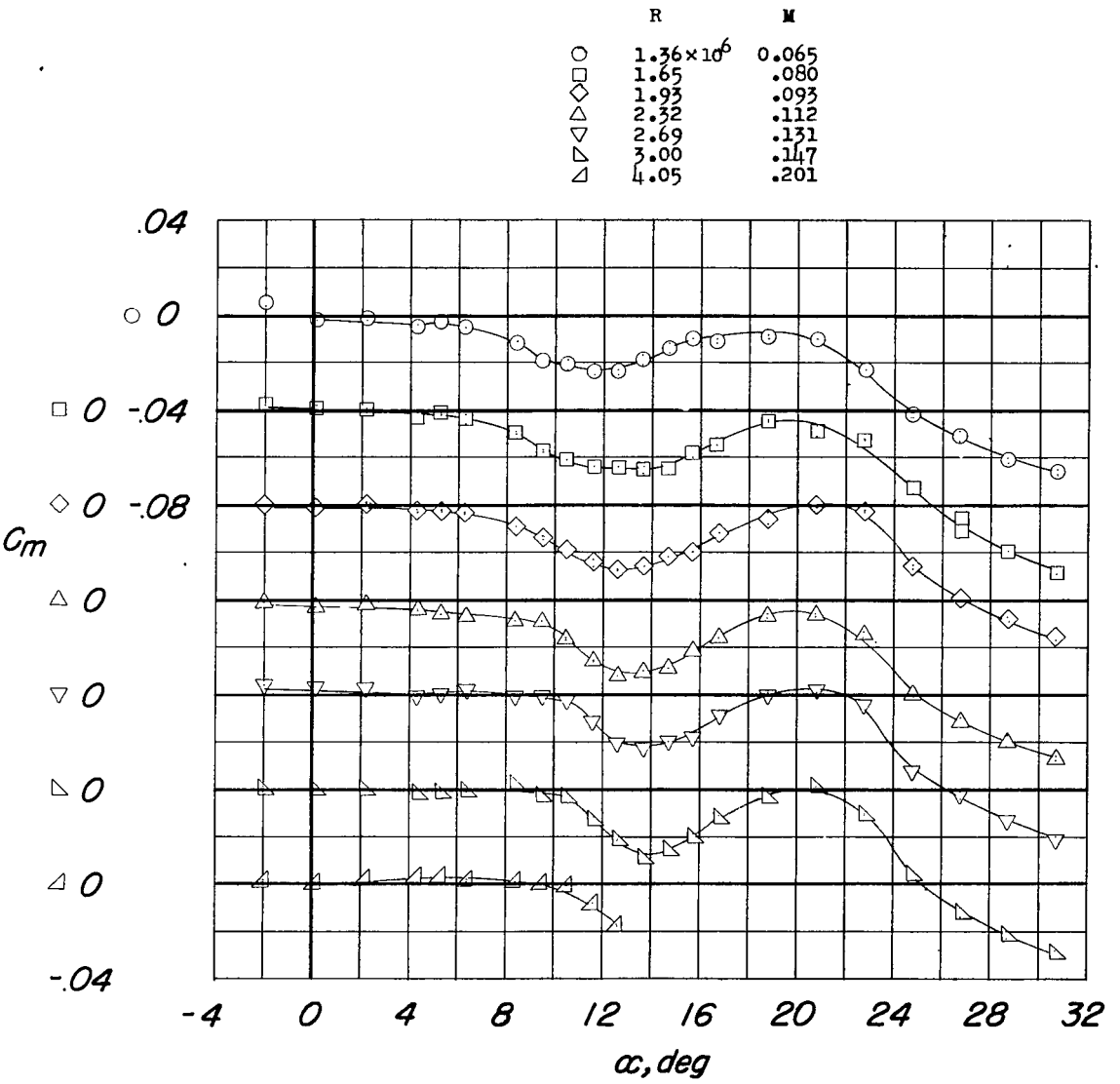

(c) C_m against α; tunnel pressure, atmospheric.

Figure 4.- Continued.

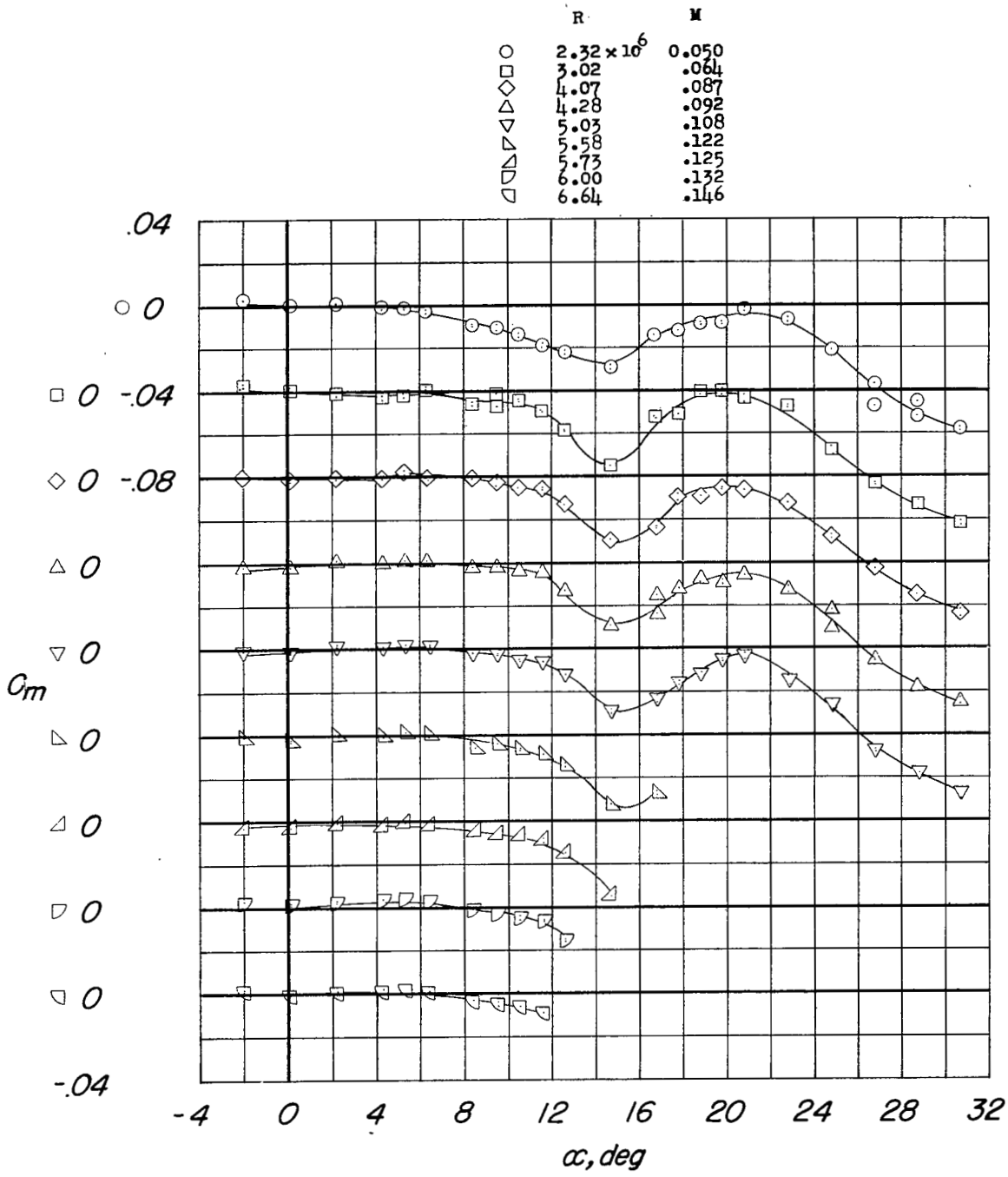

(d) C_m against α; tunnel pressure, 33 pounds per square inch, absolute.

Figure 4.- Concluded.

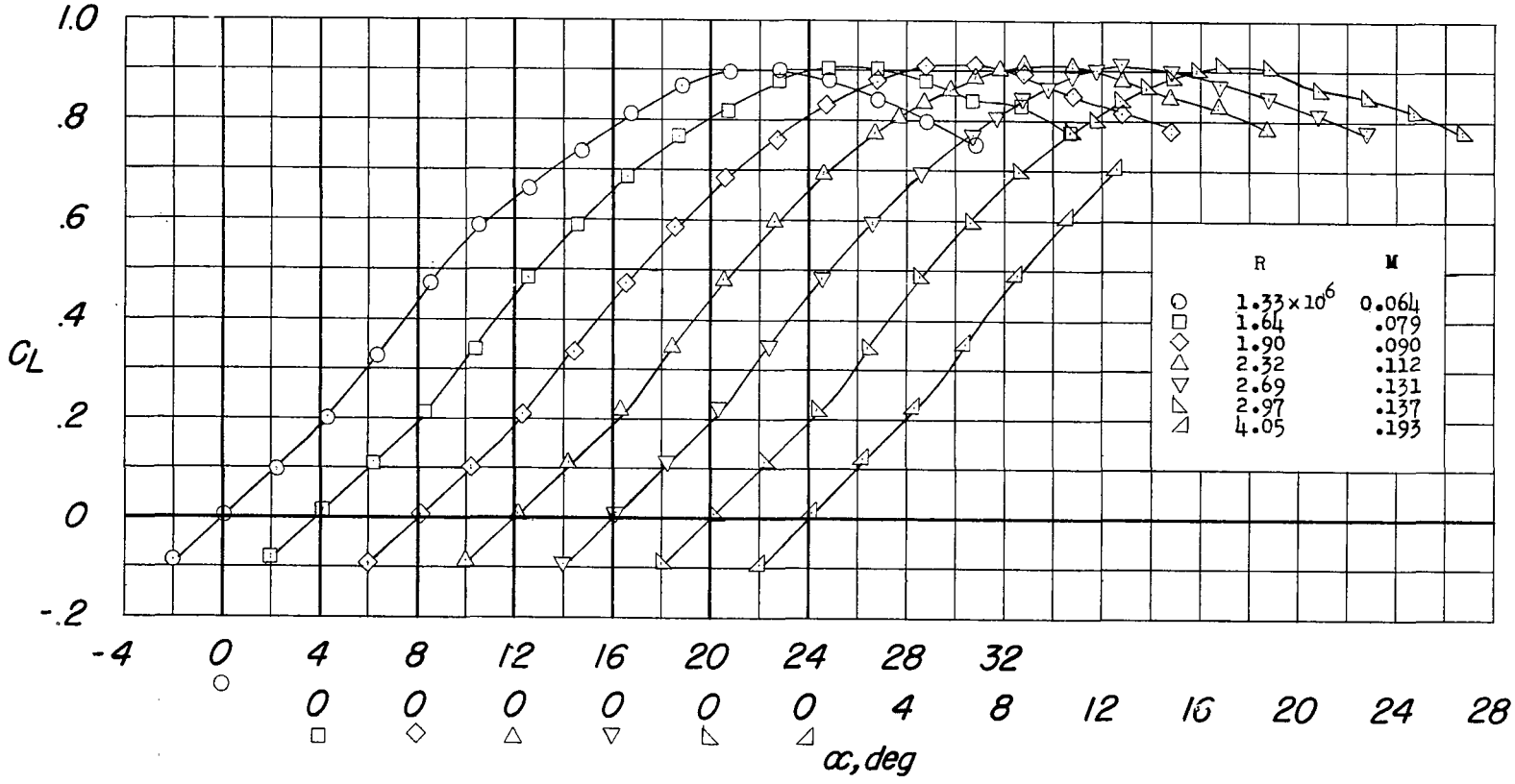

(a) C_L against α; tunnel pressure, atmospheric.

Figure 5.- Variation of lift and pitching-moment coefficients with angle of attack of a 45° sweptback wing with aspect ratio of 3 and NACA 0006-(3.88)3 modified airfoil sections. Leading-edge radius, 0.0025.

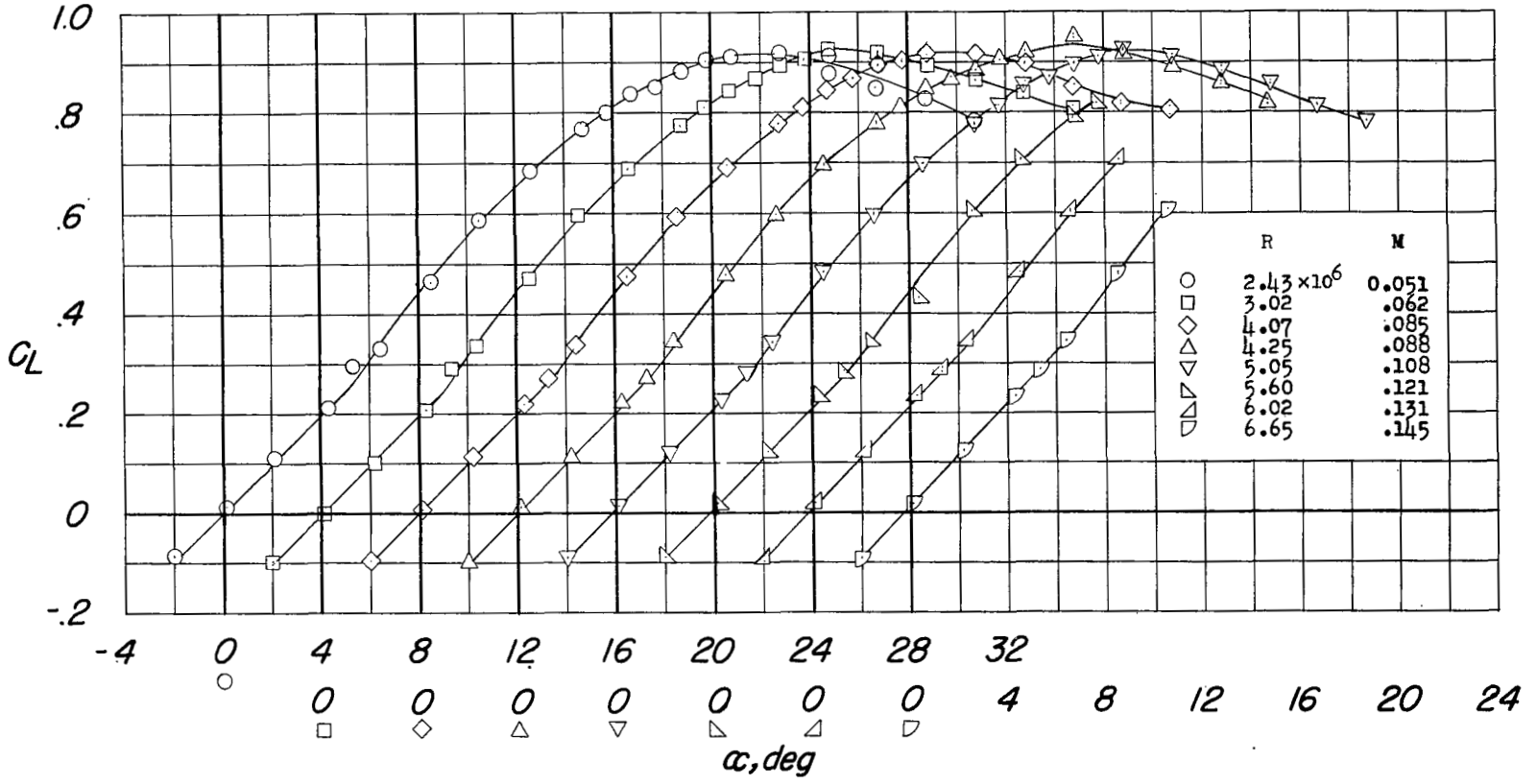

(b) C_L against α; tunnel pressure, 33 pounds per square inch, absolute.

Figure 5.- Continued.

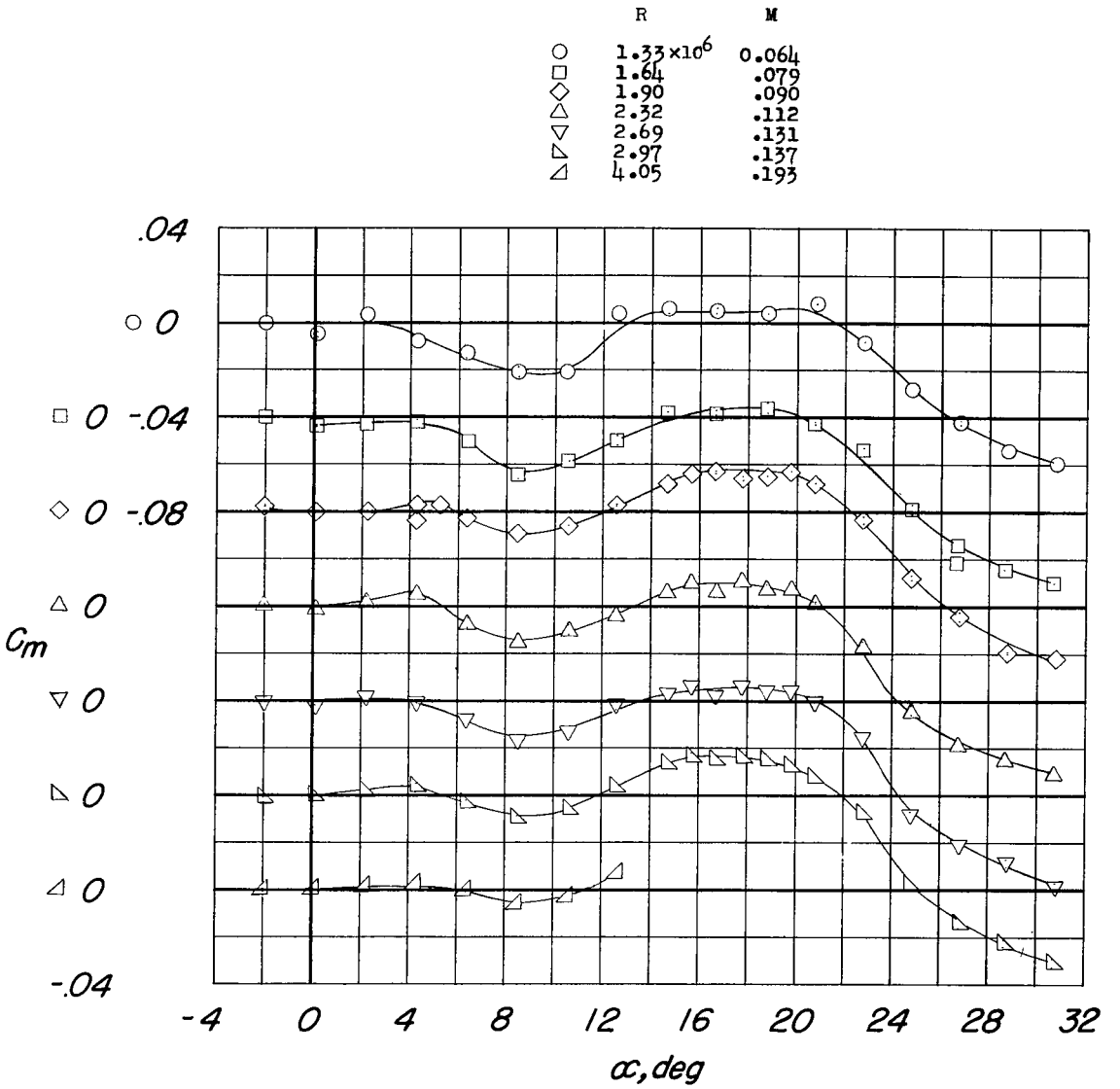

(c) C_m against α; tunnel pressure, atmospheric.

Figure 5.- Continued.

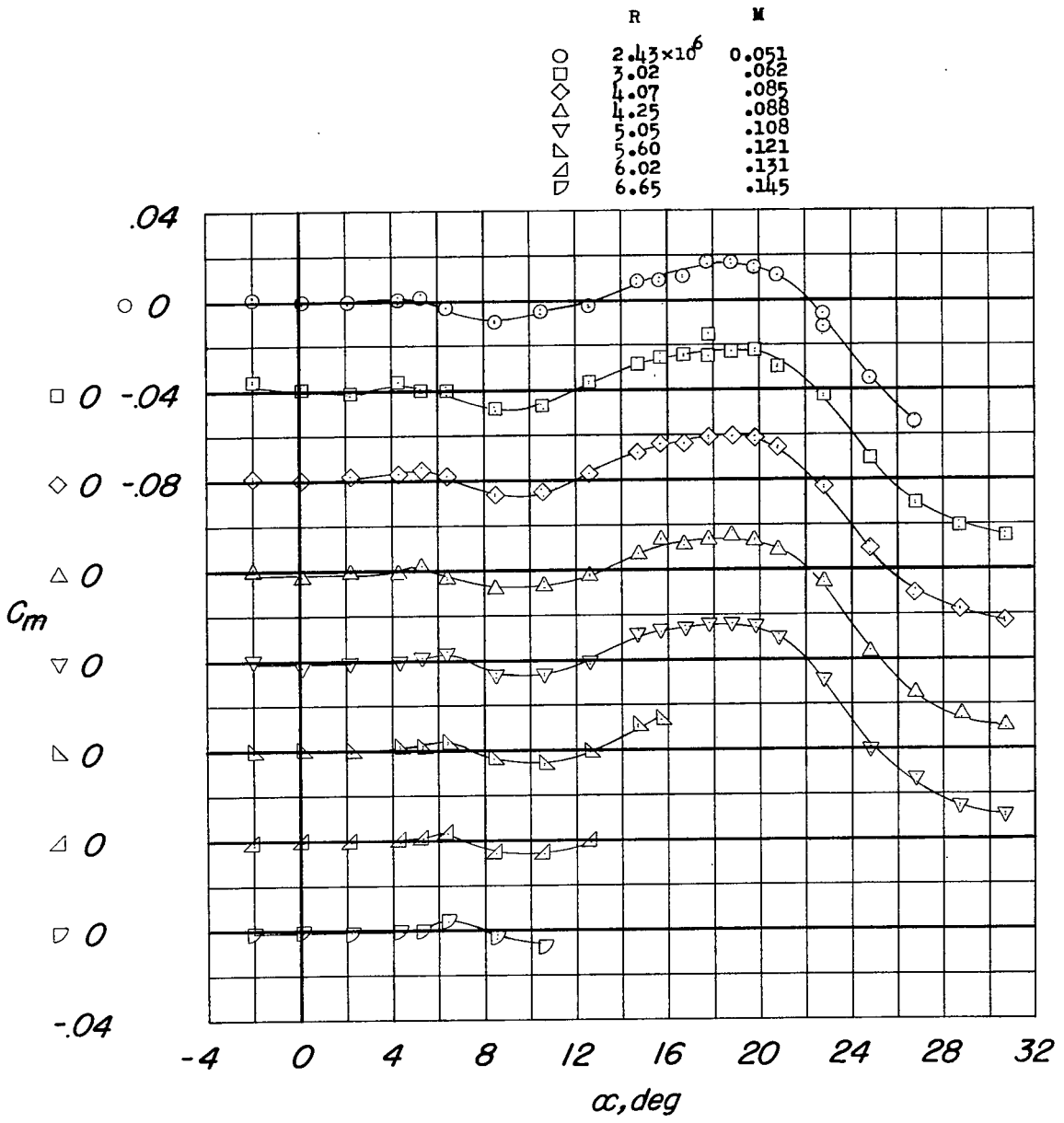

(d) C_m against α; tunnel pressure, 33 pounds per square inch, absolute.

Figure 5.- Concluded.

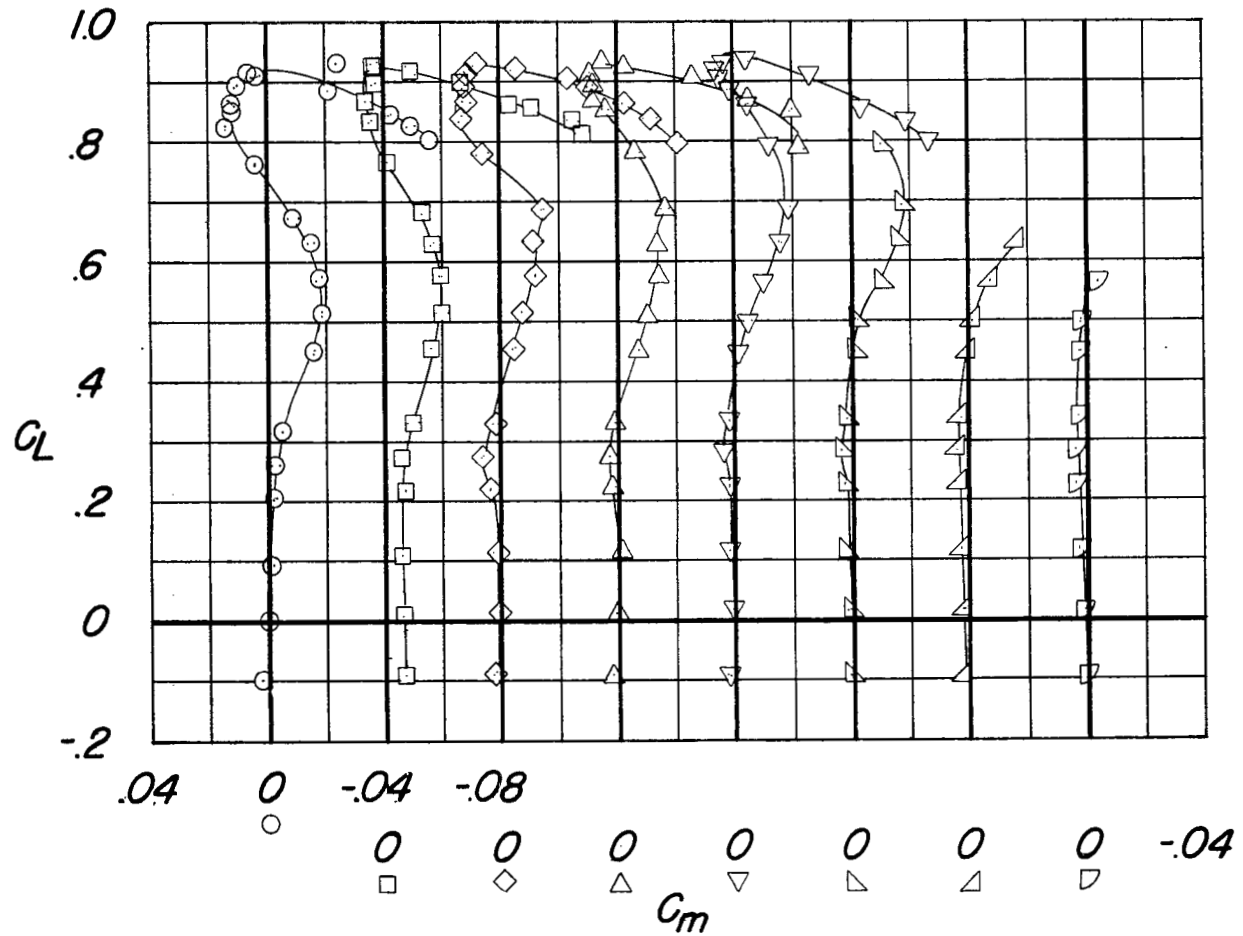

Figure 6.- Variation of pitching-moment coefficient with lift coefficient of a 45° sweptback wing with aspect ratio of 3 and NACA 0006-(4.76)3 airfoil sections. Leading-edge radius, 0.0025; tunnel pressure of 33 pounds per square inch, absolute.

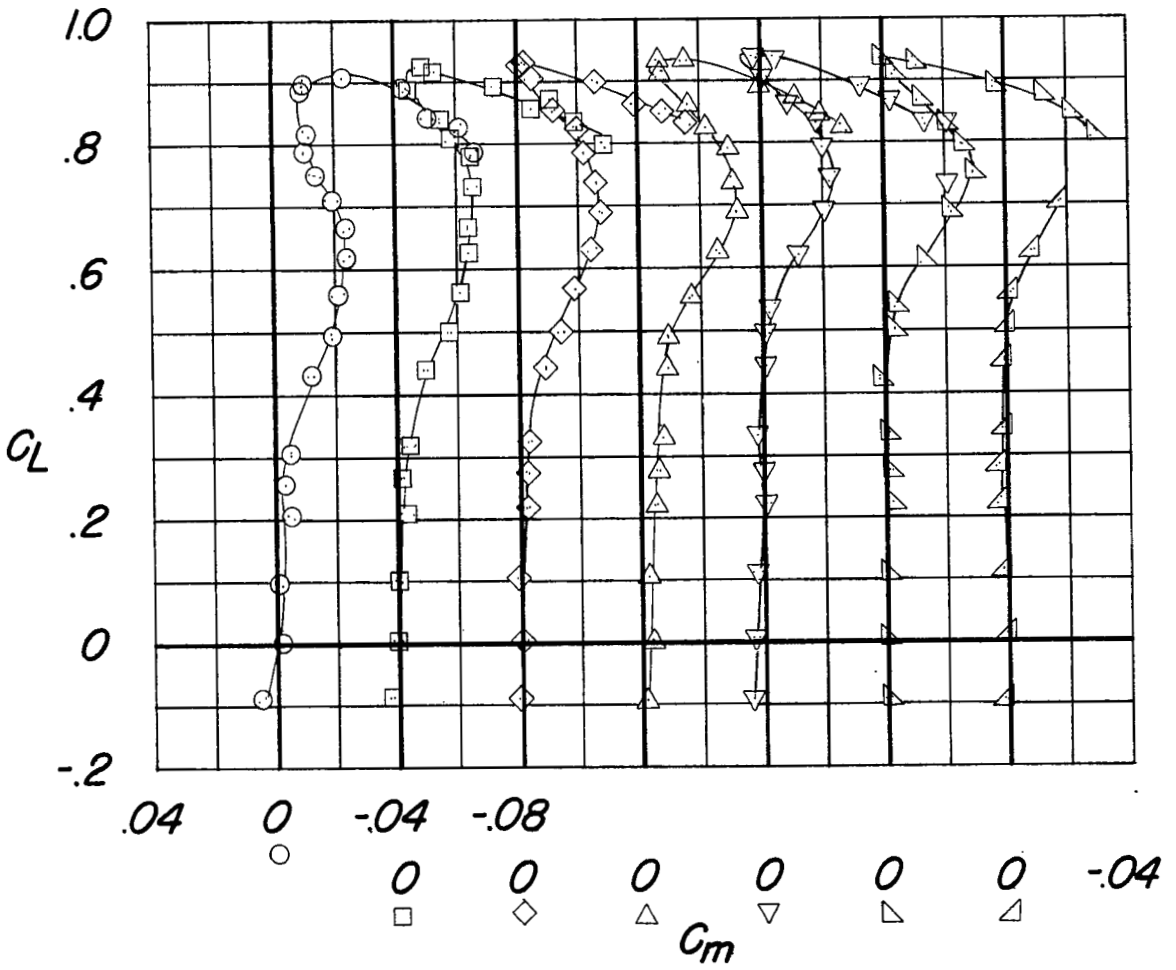

(a) Tunnel pressure, atmospheric.

Figure 7.- Variation of pitching-moment coefficient with lift coefficient of a 45° sweptback wing with aspect ratio of 3 and NACA 0006-(6.74)3 airfoil sections. Leading-edge radius, 0.0050.

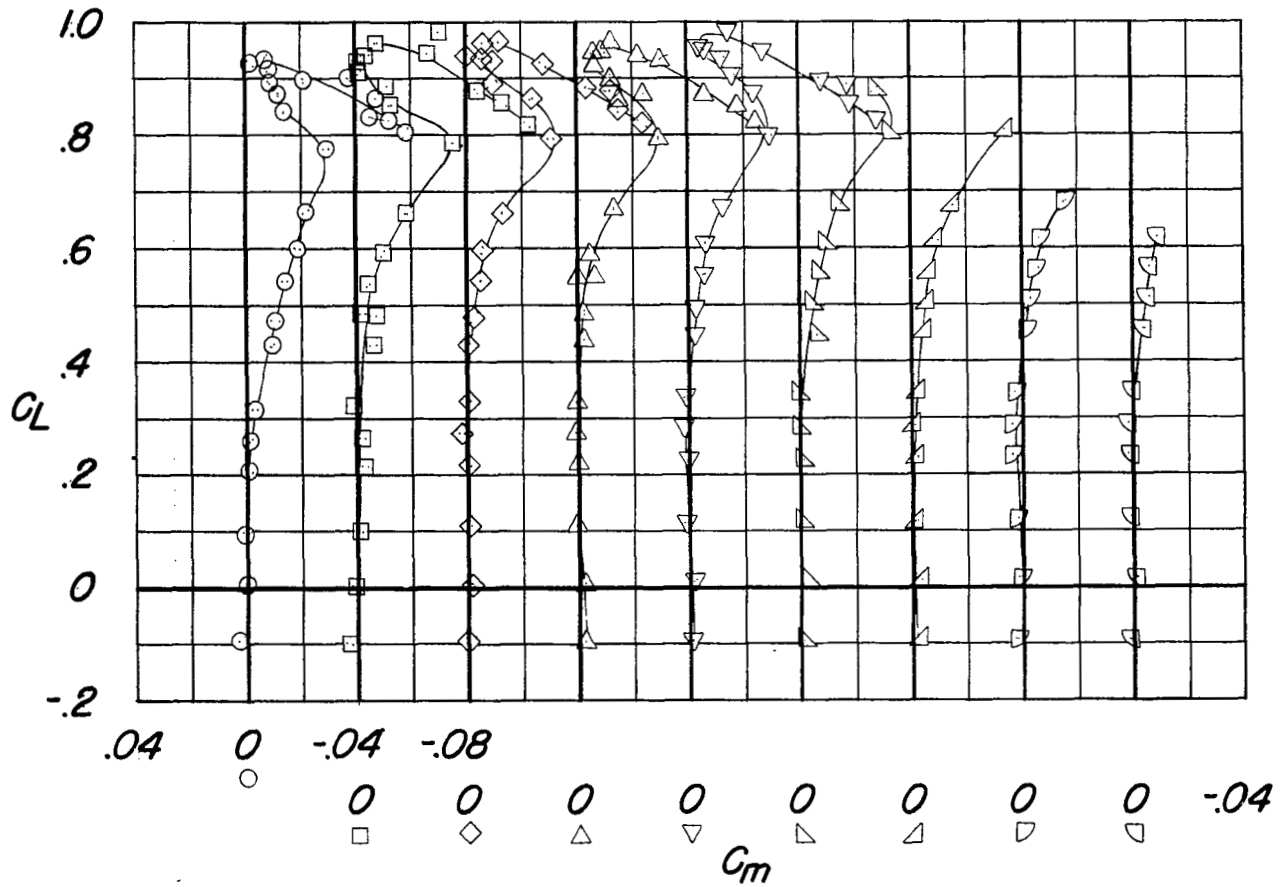

(b) Tunnel pressure, 33 pounds per square inch, absolute.

Figure 7.- Concluded.

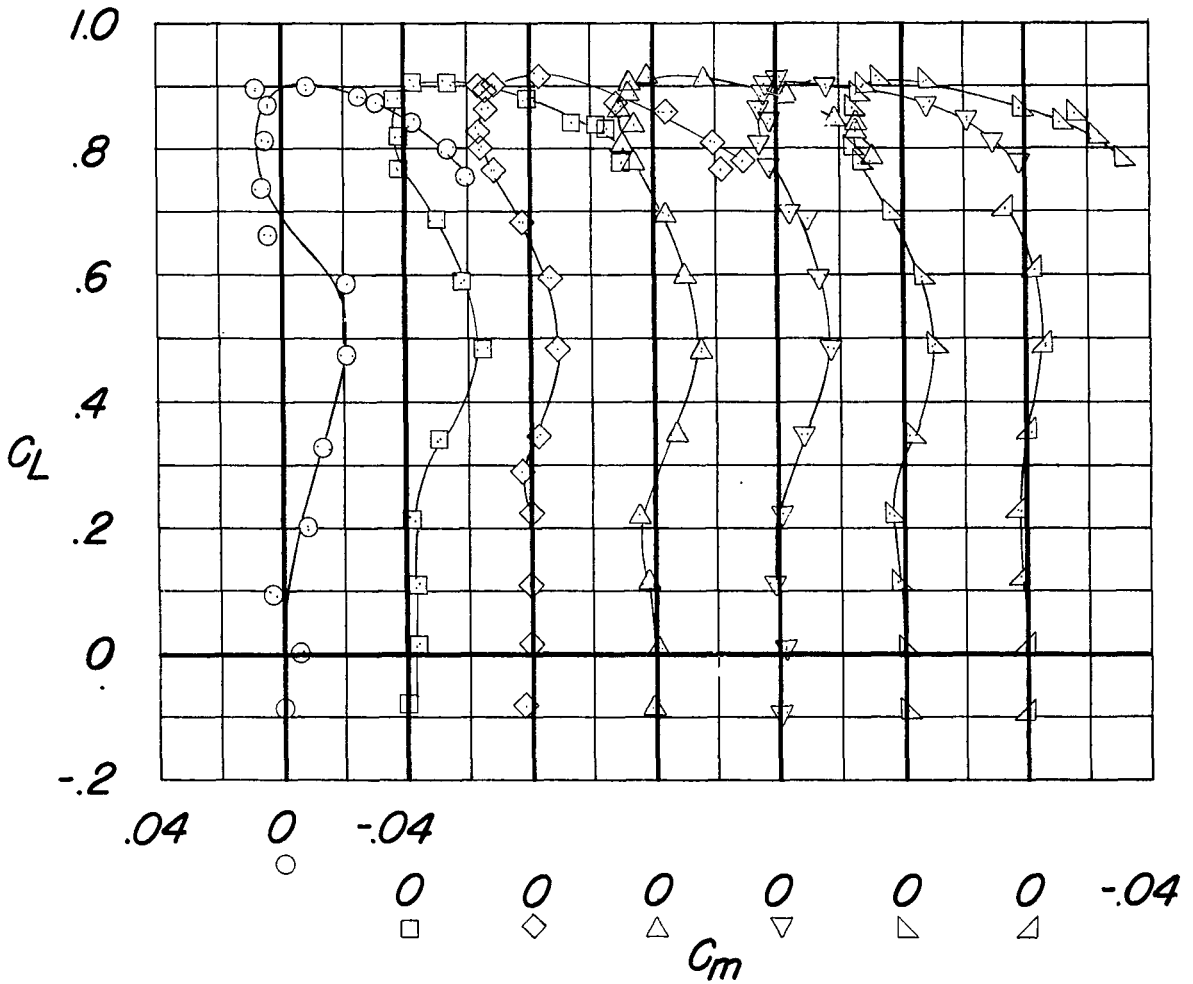

(a) Tunnel pressure, atmospheric.

Figure 8.- Variation of pitching-moment coefficient with lift coefficient of a 45° sweptback wing with aspect ratio of 3 and NACA 0006-(3.88)3 modified airfoil sections. Leading-edge radius, 0.0025.

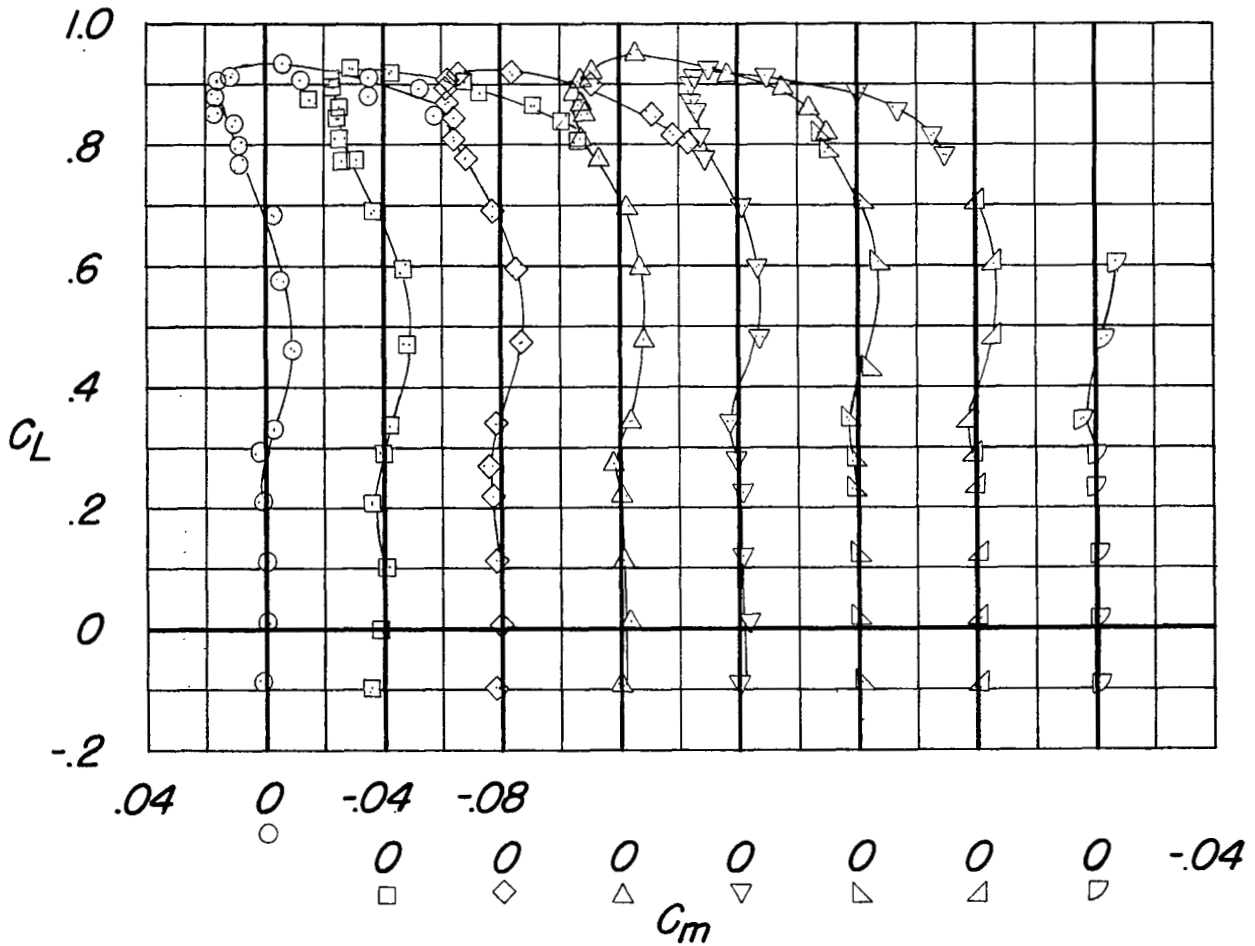

(b) Tunnel pressure, 33 pounds per square inch, absolute.

Figure 8.- Concluded.

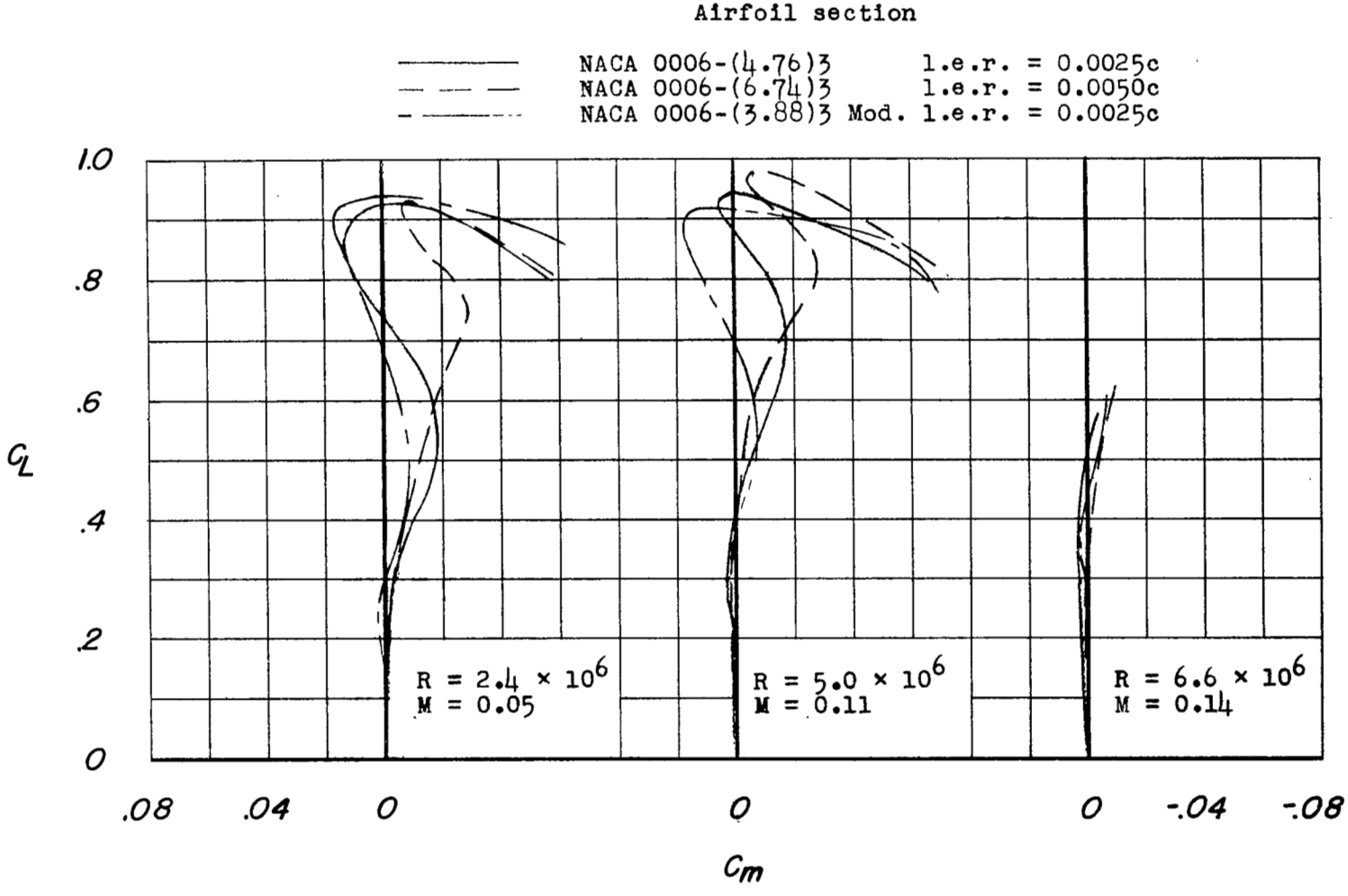

(a) Tunnel pressure, 33 pounds per square inch, absolute.

Figure 9.- Effect of changes in nose shape on pitching-moment characteristics of a 45° sweptback wing of aspect ratio 3.

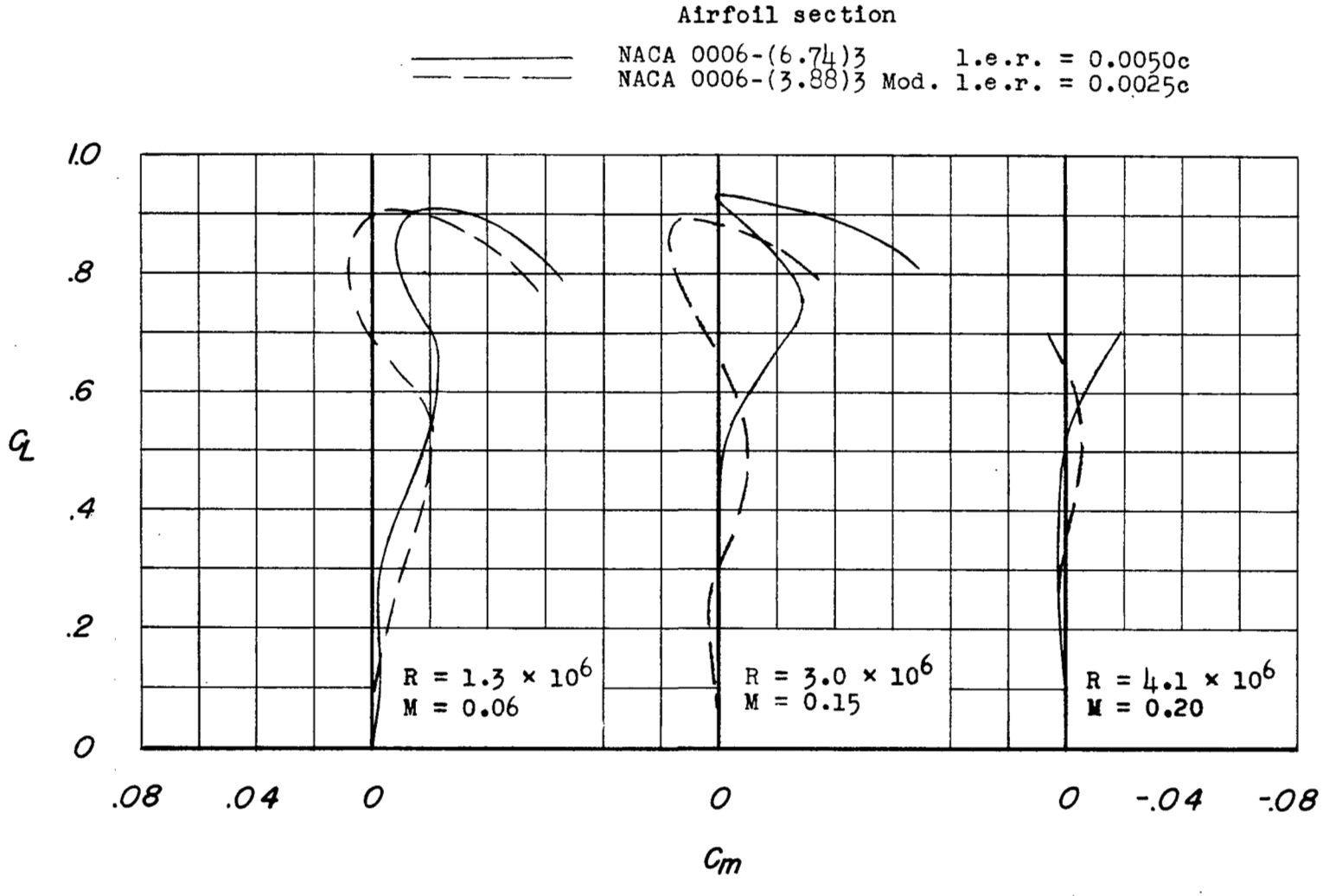

(b) Tunnel pressure, atmospheric.

Figure 9.- Concluded.

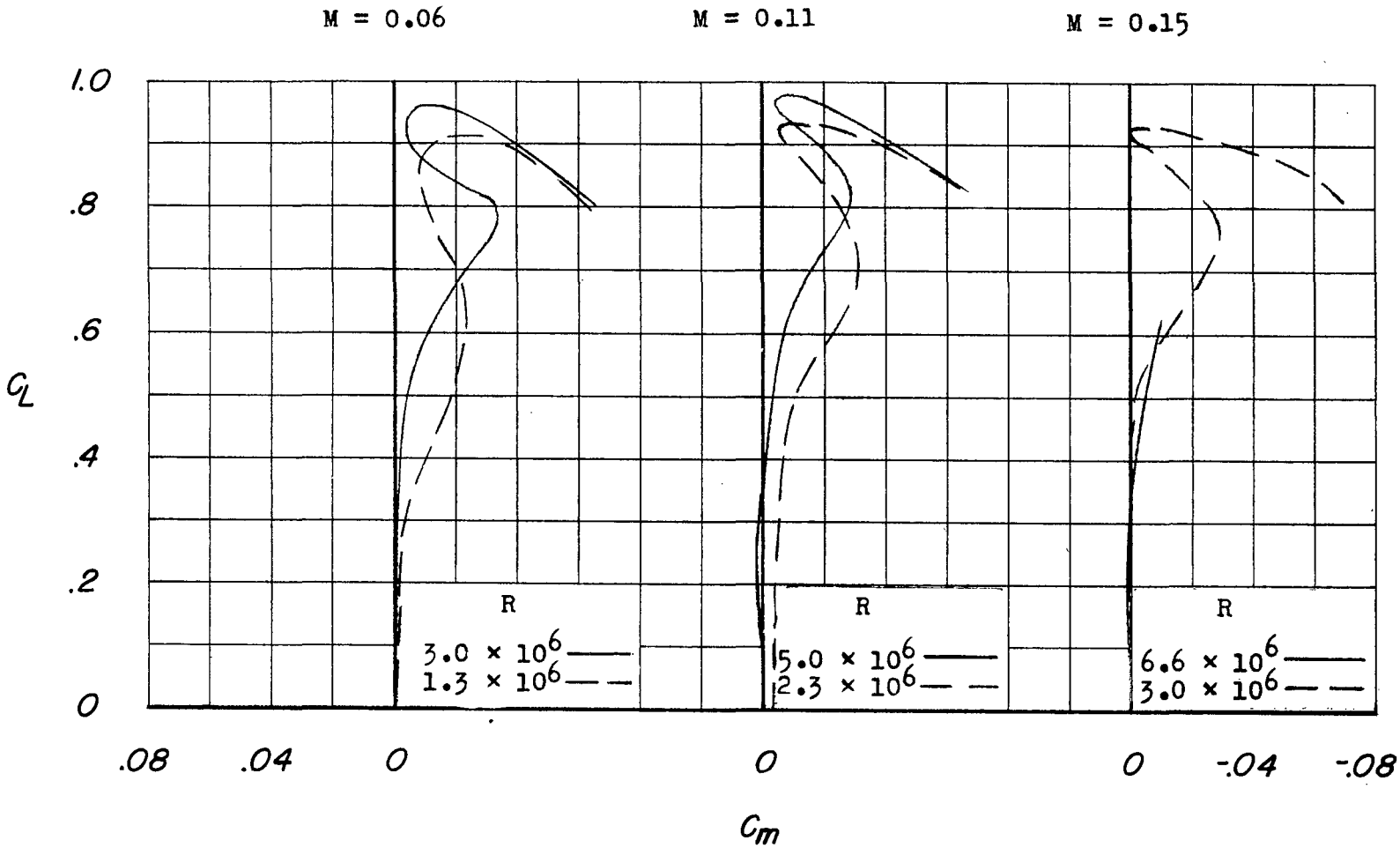

(a) Airfoil section, NACA 0006-(6.74)3; leading-edge radius, 0.0050c.

Figure 10.- Effect of Reynolds number changes on pitching-moment characteristics of a 45° sweptback wing of aspect ratio 3.

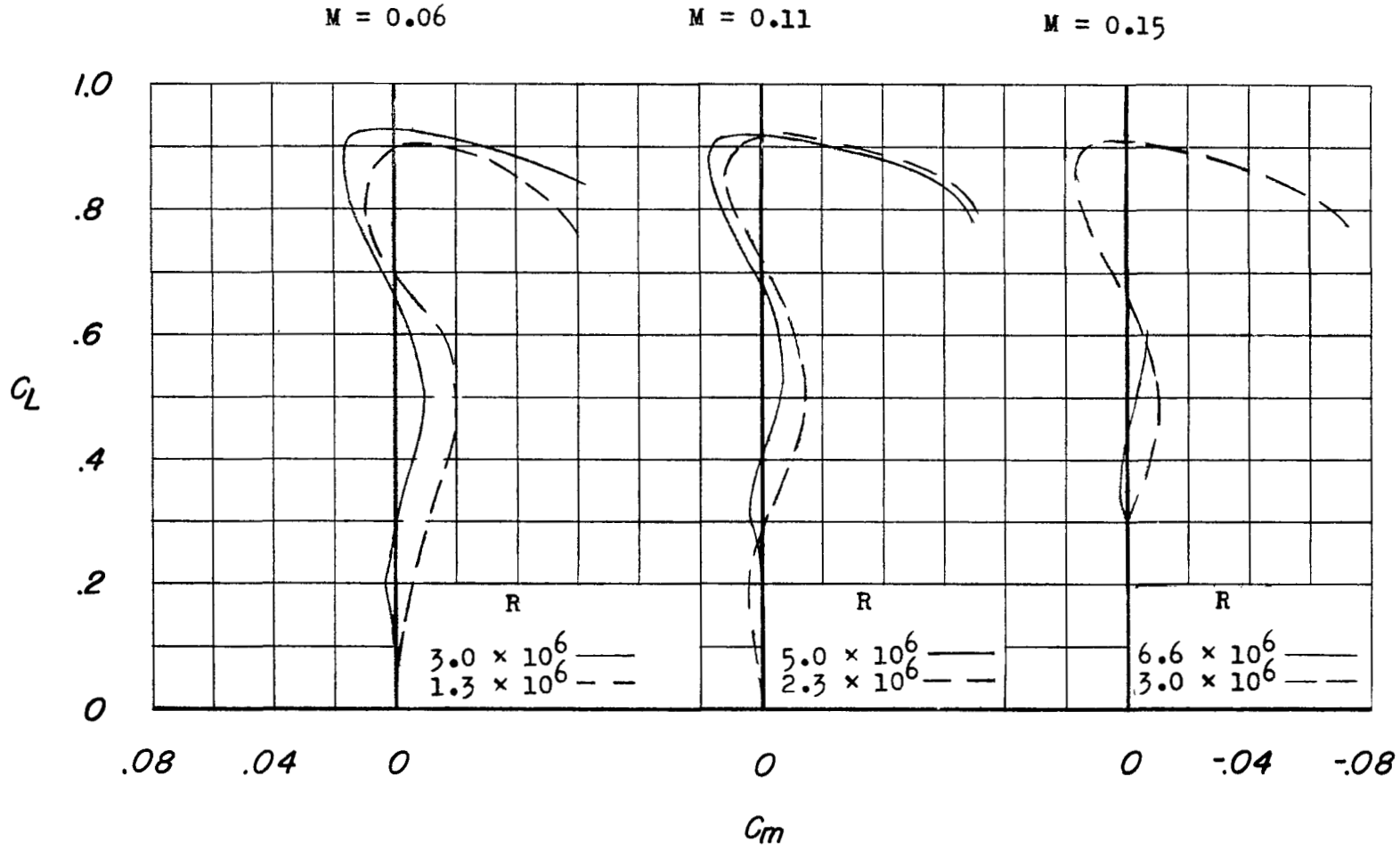

(b) Airfoil section, NACA 0006-(3.88)3 modified; leading-edge radius, 0.0025c.

Figure 10.- Concluded.

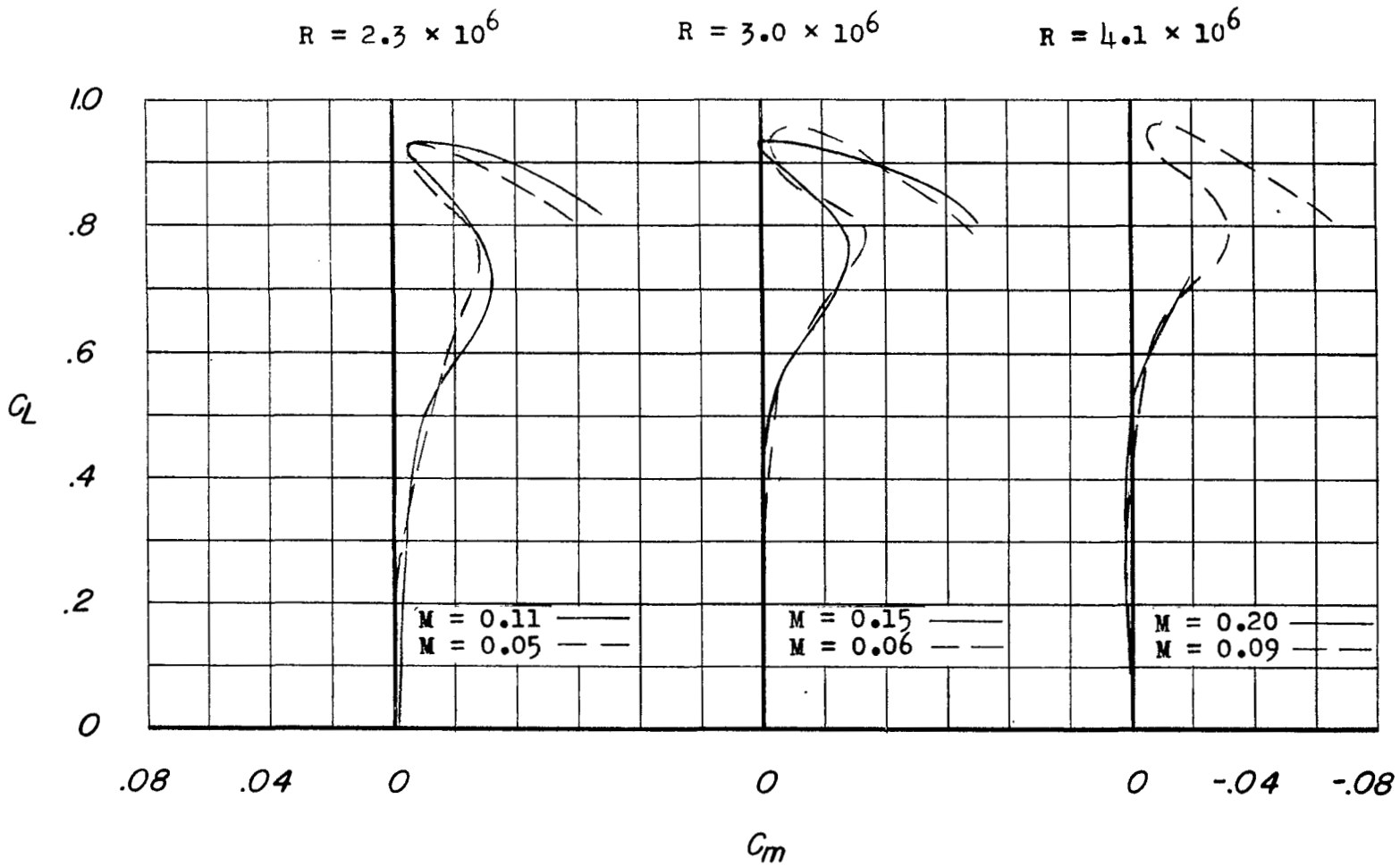

(a) Airfoil section, NACA 0006-(6.74)3; leading-edge radius, 0.0050c.

Figure 11.- Effect of Mach number changes on pitching-moment characteristics of a 45° sweptback wing of aspect ratio 3.

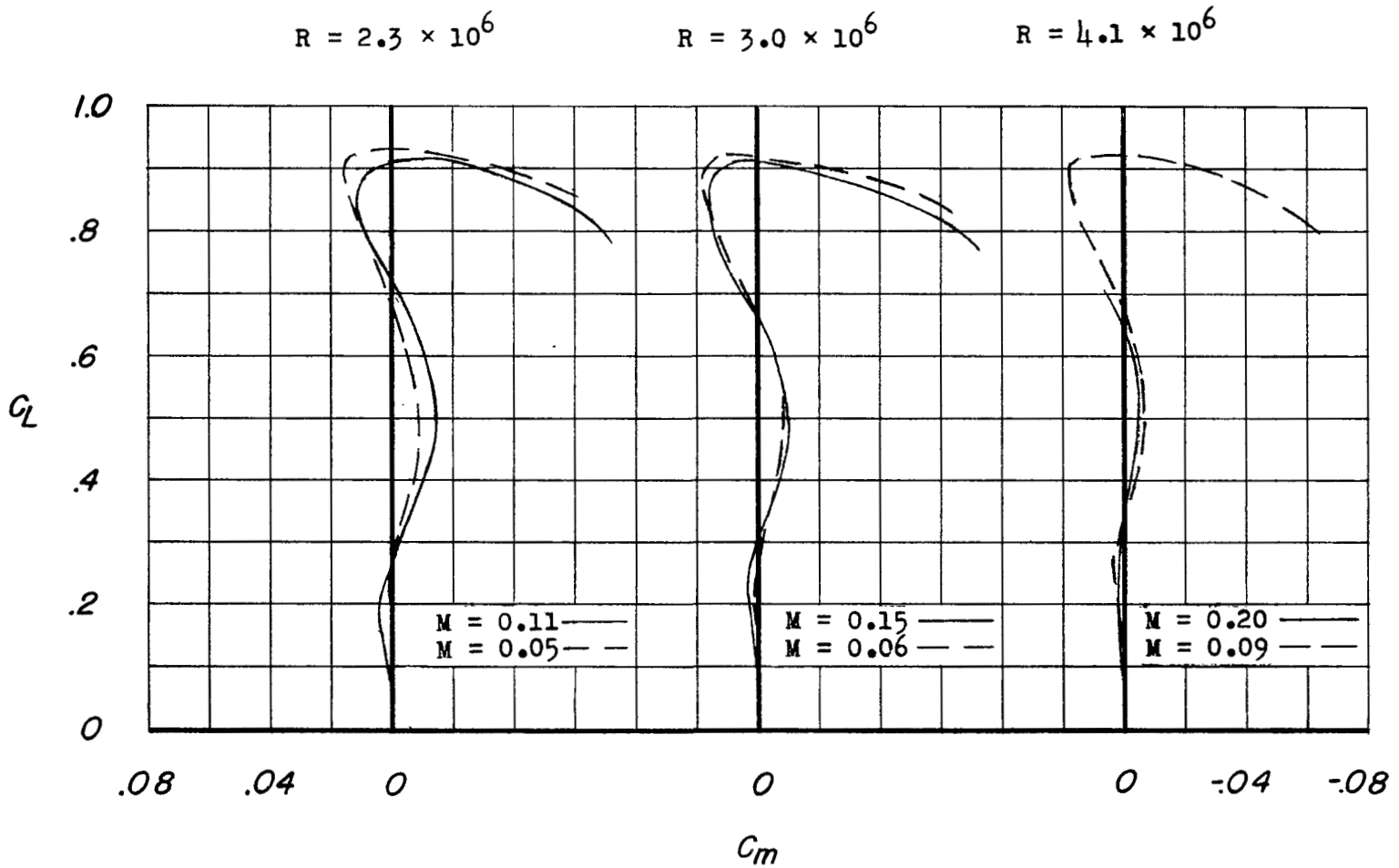

(b) Airfoil section, NACA 0006-(3.88)3 modified; leading-edge radius, 0.0025c.

Figure 11.- Concluded.

○ Tunnel pressure atmospheric.
□ Tunnel pressure 33 pounds per square inch, absolute.

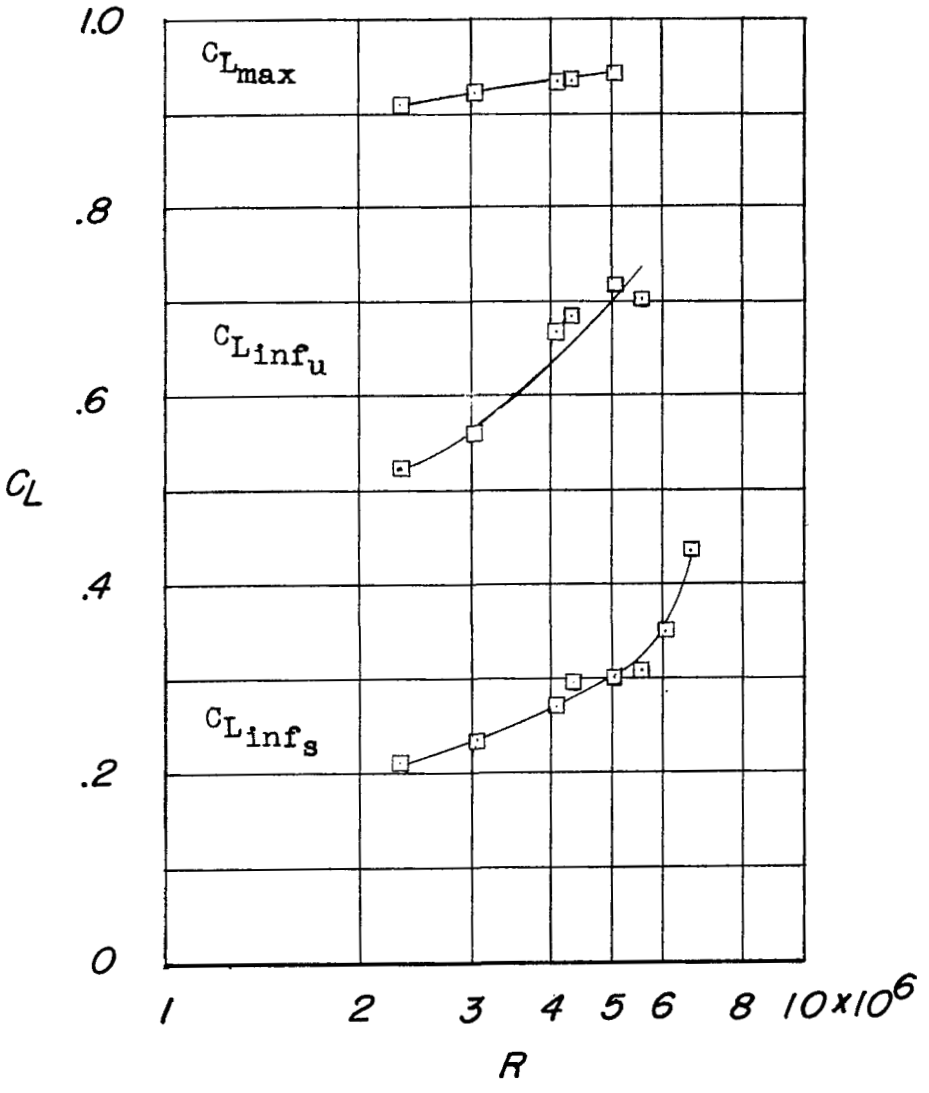

Figure 12.- Variation of inflection lift coefficients and maximum lift coefficients with Reynolds number for a 45° sweptback wing of aspect ratio 3 with NACA 0006-(4.76)3 airfoil sections. Leading-edge radius, 0.0025c.

○ Tunnel pressure atmospheric.
□ Tunnel pressure 33 pounds per square inch, absolute.

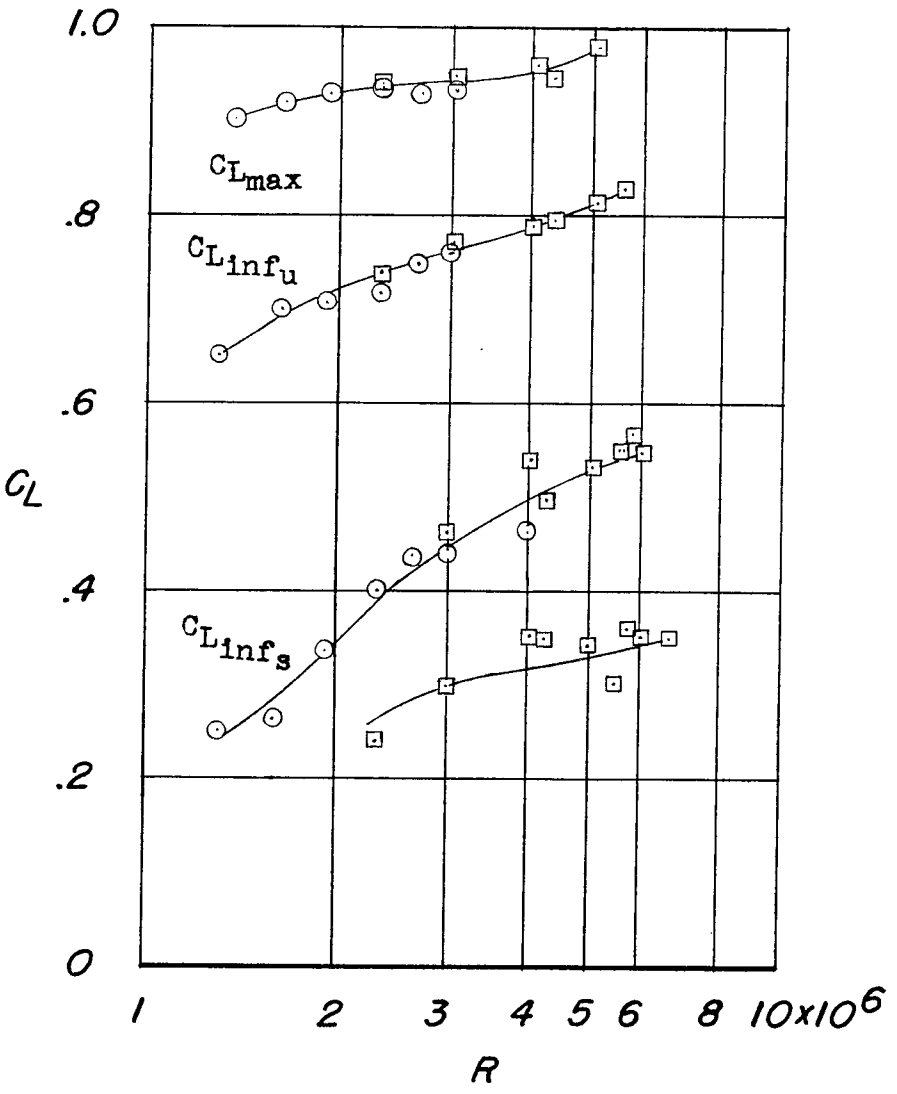

Figure 13.- Variation of inflection lift coefficients and maximum lift coefficients with Reynolds number for a 45° sweptback wing of aspect ratio 3 with NACA 0006-(6.74)3 airfoil sections. Leading-edge radius, 0.0050c.

○ Tunnel pressure atmospheric.
□ Tunnel pressure 33 pounds per square inch, absolute.

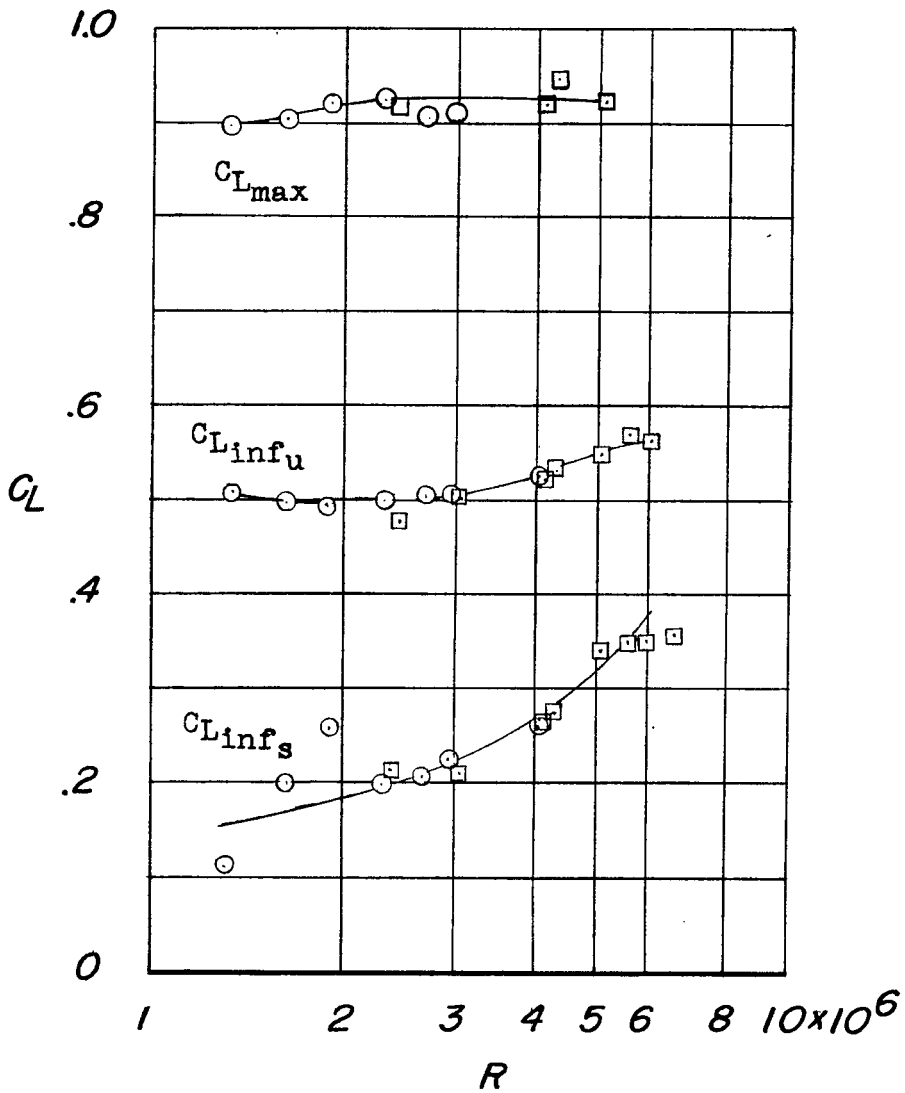

Figure 14.- Variation of inflection lift coefficients and maximum lift coefficients with Reynolds number for a 45° sweptback wing of aspect ratio 3 with NACA 0006-(3.88)3 modified airfoil sections. Leading-edge radius, 0.0025c.

NACA - Langley Field, Va.